

Surface Modification of Ethylene Propylene Diene Terpolymer Rubber by Plasma Polymerization Using Organosilicon Precursors

Christian W. Karl,* Wehid Rahimi, Stephan Kubowicz, Andrej Lang, Harald Geisler, and Ulrich Giese



Cite This: *ACS Appl. Polym. Mater.* 2020, 2, 3789–3796



Read Online

ACCESS |



Metrics & More

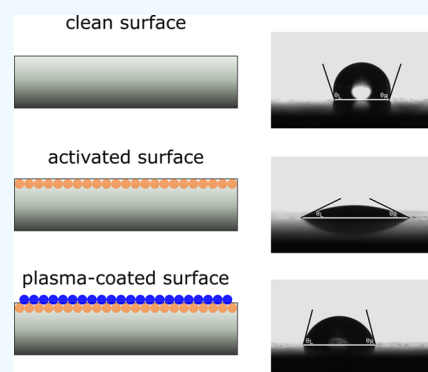


Article Recommendations



Supporting Information

ABSTRACT: The effect of atmospheric pressure plasma-enhanced chemical vapor deposition on ethylene propylene diene terpolymer (EPDM) with the precursors hexamethyldisiloxane (HMDSO) and tetraethyl orthosilicate (TEOS) on roughness, chemical composition, as well as wetting and friction properties has been investigated. For the first time, topography analyses like scanning electron microscopy, white light interferometry, digital microscopy, as well as surface analytical methods by using X-ray photoelectron spectroscopy (XPS) and time-of-flight secondary ion mass spectrometry (ToF-SIMS) were combined with contact angle and friction experiments to obtain a detailed analysis of plasma polymer surfaces. This work shows that different plasma coatings can be utilized to tailor wettability and surface energies and reduce friction of EPDM rubber, which are important for various applications. Wettability investigations have shown that both coatings are more polar compared to the untreated surface but less polar than the surface-activated EPDM without precursors. The carbon content decreased, and the content of oxygen and silicon increased after plasma polymerization, as shown by XPS investigations. ToF-SIMS investigations have revealed that the ion spectra of both coatings are very similar with a comparable surface chemistry. A lower penetration depth is considered for the contact angle measurements in contrast to the other surface-sensitive methods. The surface energy of the activated EPDM surface without precursors increases significantly compared to the untreated EPDM because of the incorporation of polar groups in the elastomer surface. Both coatings with the corresponding precursors also have a higher surface energy compared to the uncoated EPDM, whereas the TEOS coating reveals a higher surface energy than the HMDSO coating. However, both coatings have lower surface energies than the activated EPDM. The coefficient of friction and the stick–slip phenomenon can be significantly reduced using plasma polymer coatings based on organosilicon precursors sliding on glass substrates. The lowest friction values with the absence of stick–slip on EPDM were achieved by using the precursor TEOS as the friction partner.



KEYWORDS: elastomer, EPDM, plasma polymerization, analytical chemistry, surface analysis, contact angle, surface energy, friction

INTRODUCTION

Favorable mechanical properties, ozone resistance, and low cost make ethylene propylene diene terpolymer (EPDM) and similar elastomer choice materials for industrial applications such as sealings (e.g. gaskets).^{1,2} Still, elevated dry-friction coefficients accelerate the surface wear of elastomeric parts under dynamic loading. Applying lubricants (e.g. greases) and coatings to elastomeric surfaces can reduce their stick–slip friction and improve wear behavior, which, in turn, extend the lifetime of high-wear surfaces. Previous studies have investigated the use of varnish coatings as well as various chemical and plasma treatments.^{3–9} Of note, plasma-enhanced chemical vapor deposition (PECVD) is a highly relevant two-step process whereby a polymeric surface is built up by introducing a precursor (or monomer) in the plasma zone. The formed plasma in the first step contains no precursor fragments and is utilized for cleaning the surface from contaminations and organic residues. Simultaneously, the plasma activates the surface which leads to an incorporation of functional groups to

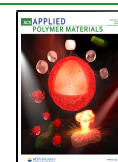
ensure the adhesion of the plasma polymerization in the second step (see Figure 1).¹⁰ Several processes occur simultaneously in this zone, namely, the formation of free radicals, fragmentation of the precursor, and recombination of fragmented molecules. The resulting surface consists of bonded thin polymeric films.¹¹

There has been very little research on the modification of elastomer surfaces via plasma polymerization with the precursors hexamethyldisiloxane (HMDSO) and tetraethyl orthosilicate (TEOS) or other organosilicon precursors to reduce friction and wear. Alba-Elias et al. and Tran et al. investigated the plasma polymerization of HMDSO and TEOS

Received: April 16, 2020

Accepted: August 19, 2020

Published: August 19, 2020



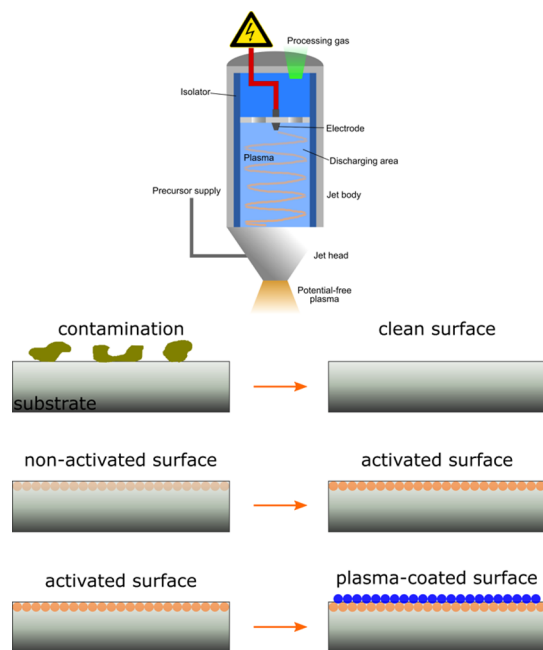


Figure 1. Fabrication process of the plasma modification of elastomer surfaces using precursors.

as precursors on EPDM.^{12,13} The properties of the plasma coatings were shown to depend on the degree of composition achieved by the precursor during the gaseous phase of the plasma. Furthermore, Verheyde et al. have shown that coatings on hydrogenated nitrile butadiene rubber (NBR) lead to a reduction of friction using (3-aminopropyl)triethoxysilane as a precursor.¹⁴ Schmidt and Paulkowski have found that friction and wear of HMDSO plasma-polymerized coatings on elastomers such as acrylic rubber, fluorocarbon elastomer, NBR, and EPDM can be reduced significantly also unlike varnish coatings.^{15–17} Furthermore, the low surface energy of EPDM is often a problem with respect to adhesion, especially in automotive applications (e.g. wipers). Hence, techniques like plasma coatings are important to improve the adhesion properties of elastomers.⁴

In this work, we used a two-step process consisting of an activation of the elastomer surface with air using atmospheric pressure PECVD (AP-PECVD) and a subsequent plasma-polymerization with the precursors HMDSO and TEOS using downstream plasma to fabricate the modified EPDM. HMDSO and TEOS are the most widely used precursors which are considered in plasma deposition systems.¹⁸ To address this issue, we investigate the deposited siloxane-based coatings of both precursors on EPDM surfaces in detail. The effects of the treatments were investigated by scanning electron microscopy (SEM), white light interferometry (WLI), X-ray photoelectron spectroscopy (XPS), time-of-flight secondary ion mass spectrometry (ToF-SIMS), contact angle measurements (sessile drop method), and surface energy calculations as well as analysis of friction properties. This will provide a better understanding about the surface properties of the organo-silicon nm-coatings on EPDM which is essential in tailoring the coatings for low-friction applications.

EXPERIMENTAL METHODS

Fabrication of EPDM. EPDM was obtained from Lanxess with the trade name Keltan 4450. EPDM consists of 52 wt % ethylene, 43.7

wt % propylene, and 4.3 wt % ethylidene norbornene (ENB). The EPDM sample composition is made of 100 phr (“per hundred rubber”) Keltan 4450, 5 phr ZnO, 1 phr stearic acid, 1.5 phr sulfur, 0.8 phr *N*-cyclohexyl-2-benzthiazylsulfenamide (Vulkacit CZ/C, Lanxess), 1 phr tetramethylthiuram disulfide (Vulkacit Thiuram/C, Lanxess) as accelerators, 70 phr carbon black N 550, 40 phr carbon black N 772, and 40 phr of an aliphatic plasticizer (Sunpar 2280, Holly Frontier Refining). Filled samples were prepared in an industrial type mixer.

The samples were treated with acetone and isopropanol (both purity 99.8%, Merck) after vulcanization to remove blooming and other impurities and thus obtain a clean elastomer surface. To generate the coatings on the EPDM surface, the AP-PECVD method was used. In the first step, the EPDM surfaces were activated with air for surface cleaning and the incorporation of functional groups consisting of oxygen and nitrogen for better adhesion. In the second step, a precursor is required for the coating, which is conveyed as a liquid via a peristaltic pump in an evaporator, so that it can enter the gas phase. The carrier gas (nitrogen) transports the gaseous precursor into the plasma nozzle, where the ignited plasma fragments the precursor. Because of the flow of the ionization gas, the plasma flame with the fragmented precursor flows out of the nozzle and reacts on the surface to be coated. On the substrate, a highly cross-linked nanoscale plasma polymer (pp) layer is formed. The organosilicon precursors HMDSO (Sigma-Aldrich, purity more than 98.5%) and TEOS (Sigma-Aldrich, purity 98%) as reflected in Figure 2 were used to feed the plasma nozzle.



Figure 2. Molecular formulas of the precursors HMDSO and TEOS.

The elastomer surface was activated by AP-PECVD using a plasma jet instrument (Plasmatreater AS400 with the single nozzle type PFW 10) from Plasmatrete GmbH (Steinhagen, Germany). The fabrication process of the plasma modification is revealed in Figure 1. The ionization gas used was compressed air with a flow rate of 2000 L/h, and nitrogen with a flow rate of 300 L/h was used as carrier gas. During the plasma polymerization, the precursor is released at 30 g/h. The plasma nozzle moves with a velocity of 10 m/min at a distance of 10 mm over the rubber sample covering an area of 80 mm × 180 mm. It scans the sample with a track width of 5 mm which results in a total contact time with a plasma flame of 17 s. The generator frequency is 19 kHz. A plasma voltage of 285 V was applied. With the standard parameters used, there is a measured current of 18 A. A big advantage of this method lies in its potential to be used as a fast-inline process, which does not require interruption of production. Further details of this method are described elsewhere.¹⁹

The deposition of the plasma process has been determined by measuring the thickness of a single-deposited TEOS and HMDSO layer on silicon wafer substrates by means of atomic force microscopy (AFM) to calculate the resulting thicknesses of the pp films on EPDM, yielding 80 nm for TEOS and 107 nm for HMDSO. The AFM Dimension Icon from Bruker (Billerica, Massachusetts, USA) was used to determine the coating thickness. The investigations were carried out in the contact mode in air using a silicon cantilever (CONTR-20) from NanoWorld with a tip radius of 8 nm and a spring constant of 0.2 N/m. Several scans were performed at different parts of the samples to investigate the uniformity of the pp surfaces. The final images were measured from a scanning area of 50 μm × 50 μm with a scanning frequency of 0.1 Hz. The measurements were performed at (25 ± 1) °C and a relative humidity of 40%.

Contact Angle Measurements and Surface Energy Calculations. The measurement of contact angles with water is a common method to measure the wettability of polymer surfaces. These

measurements record information about the outermost 5 Å of the sample surface, therefore they are very surface sensitive.²⁰ The samples were treated with acetone and isopropanol (both purity 99.8%, Merck) before the measurement to remove blooming residues (e.g. accelerators) from the surface. The cleaning of the surface had no effect on surface roughness as it was shown in previous investigations.²¹ A decrease in the contact angle, caused by polar groups in the surface after the plasma treatment, usually correlates with better bonding of adhesives, and therefore, the static contact angle has often been used as an estimate of bonding quality.^{19,22} Contact angle investigations were also carried out on the friction substrate, the glass surface. A car glass from Wilhelm Karmann GmbH (Osnabrueck, Germany) was used for this purpose. The average roughness values of glass were determined from AFM measurements (50 $\mu\text{m} \times 50 \mu\text{m}$) and are around 12 nm.²³ The glass surface was cleaned with isopropanol (purity 99.8%, Merck) before the measurement. The OCA 20 apparatus (DataPhysics Instruments GmbH, Filderstadt, Germany) was used for performing sessile drop experiments.^{21,24} A droplet of defined volume (2 μL) is carefully deposited on the surface to be examined, and a drop contour image is recorded within 2 s by a CCD camera.²¹ The details of the procedure to measure the sessile drop contact angle are described elsewhere.¹⁹ Deionized water, ethylene glycol (anhydrous, 99.8%, Sigma-Aldrich), and diiodomethane (98.0%, Merck) were used as test liquids. Eight to ten individual measurements for each liquid and for each EPDM sample and the glass surface were carried out. The contact angle measurements were performed at (23 \pm 1) °C and a relative humidity of 50%. The three liquids (water, ethylene glycol, and diiodomethane) are used to calculate the surface energy according to Wu.^{25,26} This method for calculating the surface energy is mostly used for polymers with low surface energy but is also described for more polar surfaces.²⁷

X-ray Photoelectron Spectroscopy. XPS spectra were recorded on a Theta Probe ARXPS system (Thermo Fisher Scientific, Waltham, MA, USA), using monochromatic Al K α radiation with a 400 $\mu\text{m} \times 400 \mu\text{m}$ spot size. Additionally, low-energy electron flooding was used for charge compensation. The pass energy was set up at 160 eV for the survey spectra. For the high-resolution spectra of the core levels, the pass energy was 40 eV for N 1s, S 1s, Si 2p, and Zn 2p, and 20 eV for C 1s and O 1s. Spectral processing was carried out using Casa XPS computer software. For peak fitting, a Shirley type background was used, and the C–C component of the C 1s peak at 285 eV was used to calibrate the binding energy axis.

Time-of-Flight Secondary Ion Mass Spectrometry. ToF-SIMS analysis was performed on the as-prepared EPDM samples using a "TRIFT V nanoTOF" instrument (Physical Electronics, Chanhassen, MN, USA) equipped with a 20 keV C60⁺ source. The bunched, primary C60⁺ ion beam was scanned over an area of 400 $\mu\text{m} \times 400 \mu\text{m}$ under static conditions (total ion dose < 1 $\times 10^{12}$ ions/cm²). Positive and negative secondary ion spectra were collected from 0 to 1850 *m/z*. Charge compensation was achieved by flooding the sample surface with low-energy electrons and in positive polarity additionally with 10 eV Ar⁺ ions. The mass scale of the positive and negative ion spectra was calibrated using the CH₃⁺, C₂H₃⁺, and C₃H₅⁺ peaks and CH⁻, C₂⁻, and C₃⁻ peaks, respectively, before further analysis.

White Light Interferometry. The topography and surface roughness of the EPDM samples before and after plasma treatment were measured by WLI using a Wyko NT9800 instrument (Veeco Instruments, Plainview, NY, USA). Data were evaluated using the visualization and analysis software tool Gwyddion 2.53.

Digital Microscopy. The topographies of the TEOS and HMDSO plasma-modified elastomer surfaces were determined using the digital microscope system VH6-600 with the standard zoom lens VH-Z20R at 200 \times magnification (Keyence, Osaka, Japan).

Scanning Electron Microscopy. Surface morphologies of the treated EPDM samples before and after the friction measurements were examined on a Zeiss EVO MA 10 scanning electron microscope (Carl Zeiss AG, Oberkochen, Germany), which was operated at 7 keV

for electron imaging with a tungsten filament. A secondary electron detector was used.

Tribological Tests. For friction investigations, a modified setup of an universal testing machine 1445 build by Zwick (Zwick Roell, Ulm, Germany) was used.²¹ Friction measurements were conducted at (23 \pm 1) °C and 50% humidity on a glass substrate, which was priorly cleaned with isopropanol. Samples were cleaned before use as discussed above. Rectangular elastomer samples of 5 cm \times 5 cm with 2 mm thickness were put under a constant normal force F_N of 30 N, resulting in a nominal load of 12.3 kPa and drawn at various stationary velocities between 0.01 and 30 mm/s horizontally over the substrate. To determine the coefficient of friction $\mu = F_f/F_N$, the friction force F_f acting against the sliding direction was measured. Additionally, in order to put all surfaces into a comparable state, all samples were moved over the substrate for a limited but defined time until further friction did not change the surface behavior significantly. This ensures that the contact conditions during further friction investigations were kept stable.

RESULTS AND DISCUSSION

Roughness. The surface roughness of the samples was determined by WLI, and the resulting height distributions of the used samples are represented in Figure S1. The plasma polymerized EPDM surfaces have a very similar surface roughness and are smoother than the untreated EPDM surface. The arithmetical mean height (S_a)²⁸ of the coated surfaces was calculated from the WLI data and yields 0.52 μm for HMDSO and 0.51 μm for TEOS. The untreated surface has a S_a of about 1 μm . These roughness values are in accordance with values of smooth elastomer surfaces as shown previously.²⁹ The fractal dimension, calculated from the WLI data by the box-counting method, is for all three surfaces very similar with values between 2.1 and 2.3. Nonomura et al.³⁰ have shown that the fractal dimension values obtained by the box-counting method were in the range of 2.1 for fractal urethane and silicone surfaces which are in good accordance with our values obtained by weight light interferometry measurements.

Figure 3 shows representative scanning electron micrographs of the EPDM–TEOS and the EPDM–HMDSO surface. A

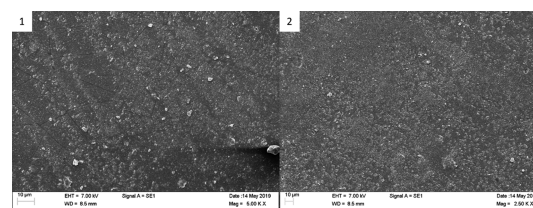


Figure 3. Scanning electron micrographs of the modified EPDM surfaces: atmospheric plasma treatment and plasma polymerization with TEOS as precursor (1) and atmospheric plasma treatment and plasma polymerization with HMDSO as precursor (2).

surface layer of the plasma film with a characteristic structure can be observed. The surface layer structure of both plasma films is very similar. These images are shown at a magnification of 5000 \times and are representative of the overall surface of the pp layer.

Contact Angle Measurements and Surface Energy Calculation. After activation treatment of the EPDM surface by atmospheric plasma, a significant decrease of the contact angle is observed, which can be attributed to the incorporation of oxygen functional groups into the EPDM surface (see Figure 4). Plasma polymerization of HMDSO and TEOS after

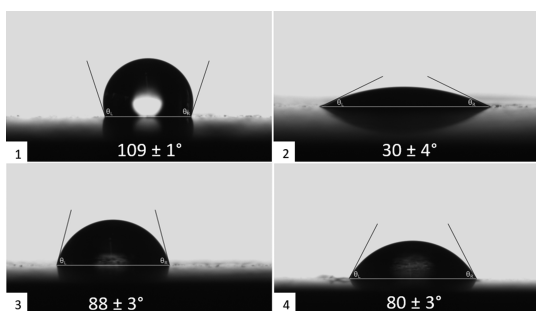


Figure 4. Contact angles on EPDM: untreated (1), atmospheric plasma treatment (2), atmospheric plasma treatment and plasma polymerization with HMDSO as precursor (3), and atmospheric plasma treatment and plasma polymerization with TEOS as precursor (4).

the atmospheric plasma treatment results in higher contact angles compared to the sample with activation only, indicating a reduction of surface polarity by both precursors. This can be explained by the fact that in addition to oxygen, nitrogen is incorporated on the surface in form of various functionalities (amino groups, ether groups, hydroxy functions, etc.).⁹ As expected, the untreated EPDM sample is hydrophobic and exhibits the highest contact angle. When comparing the two plasma polymerized surfaces, the TEOS sample shows a lower contact angle compared to the HMDSO sample, indicating a slightly higher polarity.

The average contact angles determined by the sessile drop technique were used to calculate the surface energy of the EPDM samples according to the method of Wu^{25,26} (see Figure S2). The total solid surface energy is the sum of the dispersion and polar forces of the solid surface. The surface energy of EPDM is quite low. Different values have been reported in literature since different EPDM types and qualities were used (pure or filled EPDM, type and amount of diene, content of additives, and the degree of cross-linking). Furthermore, there are different methods to calculate the surface energy, but it is often observed that the polar component of the surface energy depends on the choice of liquids. It can be regarded as an intrinsic property of the solid surface.⁴ We obtained a surface energy of about 22 mN/m with only a dispersive amount for the untreated EPDM surface. Similar values have been reported in the literature. Adam and Paulkowski, for instance, received a value of ca. 19 mN/m¹⁷ with the Wu method but with very low polar amount (ca. 1 mN/m) using different liquids. Husein and Chan, for instance, reported a surface energy value of 21.6 mN/m (dispersion) and 2.7 mN/m for the untreated EPDM surface.³¹ After activation of the EPDM surface, the surface energy increases (see Figure S2). In particular, the polar component of the surface energy increases significantly from 0 to 30 mN/m, whereas the dispersive component increases only from 22 to 33 mN/m. This increases the total surface energy to 63 mN/m. This is due to polar groups, such as amino, ether, and hydroxy functions, which are incorporated into the elastomer surface after plasma treatment. Both coatings with the corresponding precursors also reveal a higher surface energy than the untreated EPDM because of the higher polarity of their surfaces in contrast to the very hydrophobic EPDM surface. The TEOS coating shows a higher surface energy (45 mN/m) than the HMDSO coating (30 mN/m). Adam and Paulkowski have reported a very similar value of the surface

energy for a HMDSO pp on EPDM (29 mN/m).¹⁷ The percentage of the polar component in the total surface energy is higher in EPDM–TEOS than in EPDM–HMDSO. Possibly, this is due to the higher organic nature of the HMDSO monomer and the formed pp layer compared to TEOS.¹⁸ The surface energy of the glass used as the substrate for the friction investigations was calculated and is lower than the surface energy of the activated surface. Glass is a typical example of a strongly polar solid surface. Both, the polar and disperse parts of the surface energy of glass are lower than those of the activated EPDM sample. In the literature, the surface energy values of natural or synthetic quartz and silica films are discussed in detail. Depending on the pretreatment of a glass surface, a wide range of values between 50 and 230 mN/m has been reported.^{32–34} Surface energies for glass were calculated according to the Wu method of Zgura et al. The surface energy values of Zgura et al. are about 70 mN/m, and our values are about 53 mN/m. Because of the pretreatments, such as heating the glass, the disperse part of the surface energy can be changed significantly, and the polar part is reduced by the temperature treatment as Zgura et al. have shown.²⁷ The glass we have investigated is used in automotive parts, such as car windows. The pp on the EPDM increases the surface energy and improves adhesion to the glass surface.

In previous investigations, it was shown that if the diameter of the drop is three orders of magnitude larger than the scale of the arithmetic average roughness value (R_a or S_a) of the investigated surface, the roughness has no influence on the contact angle.^{35,36} The samples used in our investigations exhibit very low S_a values (0.5–1 μm), and the drops were sufficiently larger (approx. 1.5 mm) compared to that roughness. This shows that the contact angle results are mainly determined by surface chemistry.

Surface Analysis. ToF-SIMS and XPS measurements were used to analyze the surface chemistry of the samples. The positive ion spectra of the studied sample surfaces are shown in Figure 5. As expected, the spectrum of the untreated EPDM

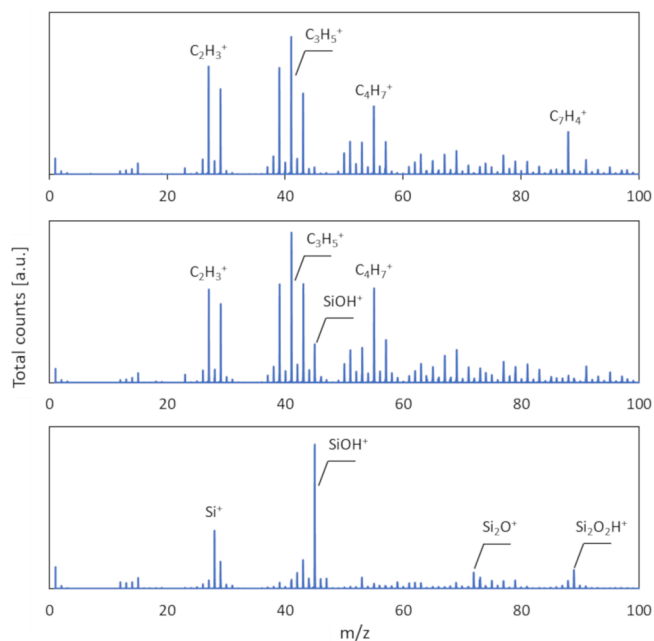


Figure 5. Positive ToF-SIMS spectra of untreated EPDM (top), EPDM–TEOS (middle), and EPDM–HMDSO (bottom).

surface shows mainly hydrocarbon ion fragments related to ethylene, propylene, and ENB, such as $C_2H_3^+$ (27 m/z), $C_3H_5^+$ (41 m/z), $C_4H_7^+$ (55 m/z), and $C_7H_4^+$ (88 m/z).³⁷ In addition, a small amount of zinc (Zn^+ , 64 m/z) was detected, which is related to the used catalyst ZnO. The positive ion spectrum of EPDM–TEOS looks very similar to the spectrum of the uncoated sample and shows many ion fragments that are associated with EPDM-related hydrocarbons. However, the mass peak at 88 m/z ($C_7H_4^+$) is significantly reduced, indicating a change in surface chemistry because of the plasma treatment and subsequent coating. Further, the characteristic ion fragment of silicon hydroxide ($SiOH^+$, 45 m/z) was detected, which is related to the plasma polymerization with TEOS. Detecting EPDM-related hydrocarbons is somewhat unexpected because the plasma polymerized surface layer should be around 80 nm, which is much higher than the detection depth, which is typically around 2–3 nm for ToF-SIMS. However, the TEOS layer thickness is significantly smaller than the surface roughness, and therefore, this finding indicates that the layer is not covering the surface completely or has some other inhomogeneities, such as pinholes. However, the microcavities and nanopores are reduced by fragmentation of the precursor molecules into small and open molecules by the plasma. Possibly, this leads to a reduction of roughness of the coatings in contrast to the uncoated EPDM surface as it was shown previously.¹²

In contrast, the spectrum of EPDM–HMDSO predominantly shows ion fragments related to silicon oxide, such as Si^+ (28 m/z), $SiOH^+$ (45 m/z), Si_2O^+ (72 m/z), and $Si_2O_2H^+$ (89 m/z). Hydrocarbon signals related to EPDM are highly reduced, which is most likely due to the higher thickness of the silicon layer on the surface compared to EPDM–TEOS.

The negative ion spectra, shown in Figure 6, are complementary to the positive spectra and reveal characteristic secondary ion fragments of silicon oxide, such as SiO_2^- (60 m/z) and SiO_3H^- (77 m/z) for both EPDM–TEOS and EPDM–HMDSO. Like the positive ion spectrum, the negative

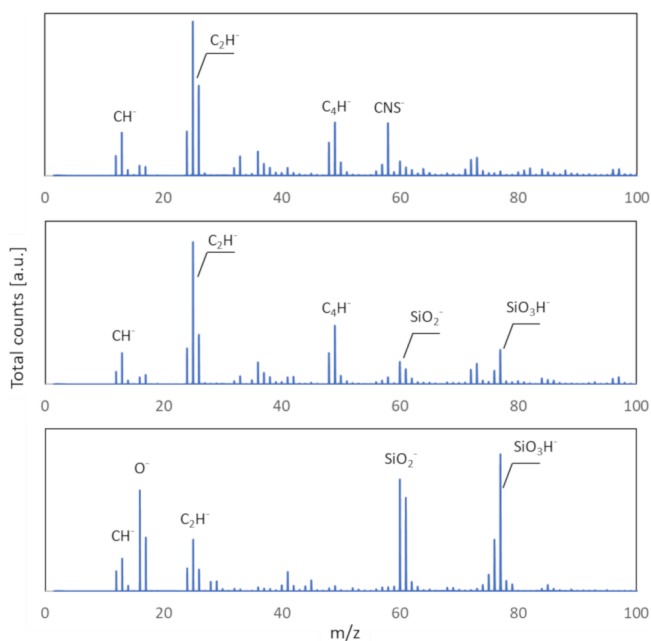


Figure 6. Negative ToF-SIMS spectra of untreated EPDM (top), EPDM–TEOS (middle), and EPDM–HMDSO (bottom).

ion spectrum of EPDM–TEOS shows also fragments of EPDM. The CNS^- ion fragment (58 m/z , residue due to vulcanization) is only present in the untreated sample. Besides the presence of EPDM in the EPDM–TEOS spectra, the ion spectra of both coatings are very similar, indicating that the chemical structure of the silicon coatings is similar. ToF-SIMS spectra in the mass range 100–200 m/z have been added to the Supporting Information, both for positive and negative ion fragments, as shown in Figures S3 and S4.

Ion maps of silicon oxide, shown in Figure S5, reveal a relatively homogeneous coating of pp-TEOS and pp-HMDSO, respectively, on top of the EPDM. However, the layer of the EPDM–TEOS sample seems to have small inhomogeneities in the form of holes, which explain the presence of EPDM fragments in the spectrum.

XPS has been used to assess the chemical composition at the surface of the untreated and plasma-polymerized EPDM rubber samples. Table 1 summarizes the results. The

Table 1. Chemical Surface Composition of the Studied EPDM Samples (at. %)

	composition (at. %)					
	C	N	O	Si	S	Zn
untreated EPDM	90.7	0.6	6.0	–	2.2	0.5
EPDM–TEOS	63.5	–	20.2	15.8	–	0.5
EPDM–HMDSO	28.1	–	39.3	32.5	–	0.1

composition of the untreated EPDM surface is in accordance with its chemical composition described in the Material Preparation section above. As expected, the plasma polymerization decreases the carbon content at the surface and increases the content of oxygen and silicon mainly because the EPDM surface is covered with a silicon oxide rich layer.

The pp-HMDSO surface contains roughly twice as much oxygen and silicon than the pp-TEOS surface, which follows the results from ToF-SIMS. Furthermore, the level of zinc in the pp-TEOS sample is higher compared to the pp-HMDSO sample. Zinc is only used in the preparation of the EPDM. The zinc is contained in zinc oxide and acts as an accelerator and activator together with the stearic acid. The higher levels of zinc in the pp-TEOS sample suggest a thinner or inhomogeneous surface layer of the pp compared to the pp-HMDSO sample (see SEM micrograph in Figure 3), which matches the results from ToF-SIMS.

A detailed peak fitting of the Si 2p spectra was carried out in order to find all components corresponding to different silicon environments (Figure S6). The Si 2p_{1/2} and Si 2p_{3/2} components of the different silicon environments were fitted with two pure Gaussian functions as it had been shown previously that they fit best for silicon oxide peaks.³⁸ The relative intensity was set to 1:2 (Si 2p_{1/2}/Si 2p_{3/2}), and the peak position and full width half maximum (fwhm) of each peak are in good agreement with the literature.³⁸ The different components of the Si 2p peak correspond to SiO (Si²⁺), Si₂O₃ (Si³⁺), and SiO₂ (Si⁴⁺). The relative proportions of the three oxidation states as well as their peak position and fwhm are summarized in Table 2. Both plasma polymerized samples have a similar proportion of the silicon environments, and most of the silicon atoms are bonded to four oxygen atoms, as in silica (SiO₂). This indicates that for both monomers the resulting pp is very similar.

Table 2. Binding Energy, FWHM, and Relative Composition of the Si-Oxidation States Present in the Samples

structure	Si-oxidation state		
	Si ²⁺	Si ³⁺	Si ⁴⁺
Si 2p _{1/2} binding energy (eV)	102.3	103.2	104.0
Si 2p _{3/2} binding energy (eV)	101.7	102.6	103.4
FWHM (eV)	1.1	1.1	1.4–1.5
Relative Composition (%)			
EPDM–TEOS	9.3	27.3	63.4
EPDM–HMDSO	10.2	26.8	63.0

When investigating the contact angle, a lower penetration depth (ca. 0.5 nm) is considered compared to the other surface-sensitive methods (XPS and ToF-SIMS, ca. 2–10 nm). As it was shown by contact angle measurements, the TEOS sample is slightly more polar than the HMDSO sample because the TEOS plasma-treated sample exhibits a lower contact angle. It was shown in previous investigations that the contact angles of polymer surfaces treated with the HMDSO plasma coating are higher compared to the TEOS plasma-treated polymers. However, the contact angle values were much higher compared to ours.¹⁸ The higher contact angle values of the HMDSO pp layer can be explained by its higher organic nature compared to the TEOS pp as shown by Kale and Palaskar.¹⁸ Fujishima et al.³⁹ have investigated HMDSO pp's on PP surfaces. It was shown that the presence of alkyl and organosilicon groups leads to a high water-repellence of the thin film.

Friction Investigations. The untreated EPDM sample and the plasma-polymerized samples with the two precursors TEOS and HMDSO were investigated regarding their friction properties. The velocity-dependent results are shown in Figure 7. The coefficient of friction for the untreated EPDM sample reveals values between 0.75 and 1.3 depending on sliding velocity, which corresponds to a typical behavior for elastomeric materials. For higher speeds, the sliding process starts to become unstable, causing pronounced stick–slip with

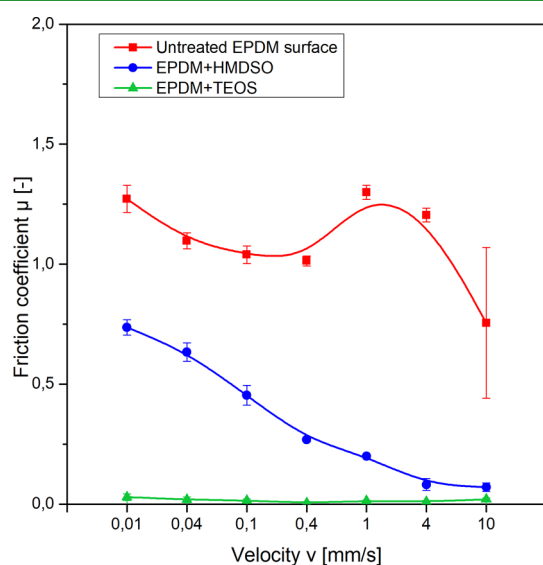


Figure 7. Velocity-dependent friction coefficient of EPDM samples: untreated surface, atmospheric plasma treatment and plasma polymerization with HMDSO and TEOS as precursors.

higher deviations of the friction values. Strongly reduced friction values can be found after the plasma polymerization procedure, which partly drop down to μ -values below 0.1. Here, the friction can be evidently reduced, especially at high velocities.

The polarity of the surfaces (see results of contact angle investigations and surface energies: Figures 4 and S2) decreases in the following order: pp-TEOS on EPDM, pp-HMDSO on EPDM, and EPDM. In contrast to the more unpolar EPDM–HMDSO sample with lower surface energy, the TEOS sample shows no stick–slip behavior and only very low friction values, which do not change if the velocity is increased. So, the TEOS coating leads to a strong decrease of the friction coefficient over the entire measuring range.¹⁷ Despite these thin layer thicknesses which lie in the range of 50–100 nm, it has been shown that the pp layer with TEOS as the precursor has significantly lower friction coefficients in contrast to the pp layer with HMDSO as the precursor, even at higher speeds.

SEM and digital microscopy micrographs of the modified EPDM surfaces with the different precursors HMDSO and TEOS before and after the friction measurement are revealed in Figures S7–S10. When comparing the SEM and digital microscopy images, no clear conclusions can be drawn as to which extend the pp layers are being abraded. Hence, further investigations on wear of both pp layers are necessary. Based on the investigations of Adam and Paulkowski concerning HMDSO pp coatings on EPDM, it has been demonstrated that the measured real contact area is significantly reduced by the plasma coating because of an increase in the surface roughness. Therefore, the reduction of the contact area has probably the most significant influence on the reduction of friction. However, the HMDSO pp coatings investigated by Schmidt and Paulkowski previously had thicknesses in the range of 0.6–4 μm and were thus significantly thicker than the coatings we investigated.¹⁵ We can confirm that the surface energies and especially the polar components are significantly increased after the plasma treatment as it is reported in the literature before.¹⁷

However, the influence of the surface energy of the TEOS and HMDSO coating on EPDM has probably less influence on the friction as stated by Adam and Paulkowski.¹⁷ But this must be confirmed by further investigations. Moreover, further experiments must show the influence of the volume properties of elastomers on friction with surfaces having the same relative contact areas.

SUMMARY AND CONCLUSION

We have shown that EPDM modified by AP-PECVD and a subsequent plasma-polymerization with the precursors HMDSO and TEOS result in coatings with unique wetting and low-friction properties. For the first time, surface analytical methods were combined with contact angle and tribological investigations in order to obtain a better understanding of the composition of the pp layers on EPDM and their fundamental surface properties. Both samples have similar roughness and fractal dimension values. Plasma polymerization of HMDSO and TEOS after the atmospheric plasma treatment results in higher contact angles compared to the sample after the activation of the elastomer surface with air.⁹ This is due to a lower polarity of the surfaces with pp coating.

The surface energy of the plasma coatings using TEOS and HMDSO increases the surface energy compared to the

untreated EPDM surface. Consequently, the plasma-treated sample without the precursor shows the highest increase in surface energy of all EPDM samples because of the incorporation of functional groups consisting of oxygen and nitrogen.

As experiments have shown, the measured friction coefficients for the plasma-coated EPDM samples were attributed to the plasma coating itself. The friction values of the EPDM–TEOS sample are lower compared to the EPDM–HMDSO sample.

The friction values can be significantly reduced when using glass as the substrate and EPDM–TEOS as the friction partner because of the more reduced contact area. However, investigations related to the wear of the pp layers on EPDM were not matter of this study. We have observed that only the untreated EPDM surface shows a very low surface energy. The incorporation of O and Si confirmed by XPS investigations reveals an increase in the surface energy of the TEOS and HMDSO pp on EPDM. Our calculated values for the surface energies with respect to the untreated EPDM and the HMDSO pp on EPDM were in good accordance with the values which were reported in the literature. However, as it was discussed in the literature, the surface structure is modified by the plasma polymerization, and the calculated surface energies may be a complex function of the functional groups and the surface structure.⁴ Further investigations are necessary, for example, by varying the surface composition of the plasma layer on the elastomer and as well as the usage of other precursors. Additionally, we would suggest that systematic wear tests should be carried out in the future. This includes the variation of the thickness of the pp layer as well as SEM–energy-dispersive X-ray and XPS investigations before and after wear of the pp layers on EPDM. Plasma-modified EPDM surfaces with different precursors enable well-tailored elastomer composites for various technical applications, such as elastomer products (hoses, seals, wipers, and profiles) where surface modification and improved adhesion properties are important to reduce friction and wear.

■ ASSOCIATED CONTENT

SI Supporting Information

The Supporting Information is available free of charge at <https://pubs.acs.org/doi/10.1021/acsapm.0c00401>.

Graphs showing the height distribution and cumulative height distribution measured by WLI; graph showing the surface energies of the different EPDM surfaces and glass; positive and negative secondary ion spectra in the mass range 100–200 m/z ; combined negative secondary ion images representing the silicon oxide layer on EPDM–TEOS and EPDM–HMDSO; graphs showing the detailed peak fitting of the Si 2p peaks of EPDM–TEOS and EPDM–HMDSO; scanning electron micrographs of the modified EPDM surfaces with the different precursors HMDSO and TEOS showing the surface structure before and after the friction measurement; and digital microscopy micrographs of the modified EPDM surfaces with the different precursors HMDSO and TEOS, showing the surface structure before and after the friction measurement (PDF)

■ AUTHOR INFORMATION

Corresponding Author

Christian W. Karl – Materials and Nanotechnology
Department, SINTEF Industry, 0373 Oslo, Norway;
✉ orcid.org/0000-0002-8797-3926; Email: cwolkfkarl@gmail.com

Authors

Wehid Rahimi – German Institute of Rubber Technology (DIK e.V.), 30519 Hanover, Germany

Stephan Kubowicz – Materials and Nanotechnology
Department, SINTEF Industry, 0373 Oslo, Norway

Andrej Lang – German Institute of Rubber Technology (DIK e.V.), 30519 Hanover, Germany

Harald Geisler – German Institute of Rubber Technology (DIK e.V.), 30519 Hanover, Germany

Ulrich Giese – German Institute of Rubber Technology (DIK e.V.), 30519 Hanover, Germany

Complete contact information is available at:

<https://pubs.acs.org/10.1021/acsapm.0c00401>

Author Contributions

The manuscript was written through contributions of all authors. All authors have given approval to the final version of the manuscript.

Funding

The research of this manuscript was financially supported by the German Federal Ministry of Economics and Technology within the framework of the program for the promotion of industrial community research and development (IGF project nos. 15810 BG and 18822 BG). Additionally, this study got internal funding from SINTEF Industry.

Notes

The authors declare no competing financial interest.

■ ACKNOWLEDGMENTS

The authors would like to thank Dr. Florian Platten (University of Dusseldorf) and Dr. Nicolas Krumenacker (SINTEF Industry) for useful discussions.

■ REFERENCES

- (1) Dutra, J. C. N.; Massi, M.; Otani, C.; De Cassia Lazzarini Dutra, R.; Diniz, M. F.; Urruchi, W. I.; Maciel, H. S.; Bittencourt, E. Surface Modification of EPDM Rubber by Reactive Argon-Oxygen Plasma Process. *Mol. Cryst. Liq. Cryst.* **2002**, *374*, 45–52.
- (2) Hopmann, C.; Dering, J. P.; Cöllen, G. Property Modification of Epdm Rubber Compounds Using Ptfе Micro Powder. *Int. Polym. Sci. Technol.* **2013**, *40*, 1–6.
- (3) Ellul, M. D.; Hazelton, D. R. Chemical Surface Treatments of Natural Rubber and EPDM Thermoplastic Elastomers: Effects on Friction and Adhesion. *Rubber Chem. Technol.* **1994**, *67*, 582–601.
- (4) Grythe, K. F.; Hansen, F. K. Surface Modification of EPDM Rubber by Plasma Treatment. *Langmuir* **2006**, *22*, 6109–6124.
- (5) Karl, C. W.; Lang, A.; Stoll, A.; Weiße, A.; Stoll, M.; Klüppel, M. Tribological properties of varnished elastomers - part 1: Characterization of the surfaces by the modified Wilhelmy method. *KGK Rubberpoint* **2012**, *65* (6), 44–49.
- (6) Momose, Y.; Takada, T.; Okazaki, S. *J. Appl. Polym. Sci.: Appl. Polym. Symp.* **1988**, *42*, 49.
- (7) Osterhold, M.; Armbruster, K. Importance of surface tension for physical paint properties. *Macromol. Symp.* **1998**, *126*, 295–306.
- (8) Wheale, S. H.; Bech, J.; Nilsson, N. H.; Badyal, J. P. S. Atmospheric Versus Low Pressure Plasma Oxidation of Rubber

Surfaces. In *Polymer Surfaces and Interfaces III*; Richards, R. W., Peace, S. K., Eds.; John Wiley & Sons Ltd., 1999; pp 285–297.

(9) Wildberger, A.; Geisler, H.; Schuster, R. H. *KGK Rubberpoint* **2007**, *24*.

(10) Roth, J. R. *Industrial Plasma Engineering: Applications to Nonthermal Plasma Processing*; CRC Press: Boca Raton, 2001; Vol. 2, p 658.

(11) Bang, S. B.; Chung, T. H.; Kim, Y. Plasma enhanced chemical vapor deposition of silicon oxide films using TMOS/O₂ gas and plasma diagnostics. *Thin Solid Films* **2003**, *444*, 125–131.

(12) Alba-Elias, F.; Ordieres-Meré, J.; González-Marcos, A. Deposition of thin-films on EPDM substrate with a plasma-polymerized coating. *Surf. Coat. Technol.* **2011**, *206*, 234–242.

(13) Tran, N. D.; Choudhury, N. R.; Dutta, N. K. Surface tailoring of an ethylene propylene diene elastomeric terpolymer via plasma-polymerized coating of tetramethyldisiloxane. *Polym. Int.* **2005**, *54*, 513–525.

(14) Verheyde, B.; Havermans, D.; Vanhulsel, A. Characterization and Tribological Behaviour of Siloxane-based Plasma Coatings on HNBR Rubber. *Plasma Processes Polym.* **2011**, *8*, 755–762.

(15) Schmidt, S.; Paulkowski, D. Plasmopolymeric coating protects elastomers against wear. *Gummi, Fasern, Kunstst.* **2017**, *70*, 184–189.

(16) Adam, A.; Paulkowski, D. Plasmopolymeric coatings - A clean alternative to sliding lacquers on elastomers. *International Rubber Conference IRC, Nuremberg, Germany*: Nuremberg, Germany, June 2015.

(17) Adam, A.; Paulkowski, D. Reibungs- und Deformationsverhalten von plasmapolymers beschichteten Elastomeren. *Tribologie Fachtagung GfT at Göttingen, Germany*: Göttingen, Germany, Sept 2019.

(18) Kale, K. H.; Palaskar, S. S. Structural studies of plasma polymers obtained in pulsed dielectric barrier discharge of TEOS and HMDSO on nylon 66 fabrics. *J. Text. Inst.* **2012**, *103*, 1088–1098.

(19) Karl, C. W.; Rahimi, W.; Giese, U.; Klüppel, M.; Geisler, H. *KGK Rubberpoint* **2018**, 19–31.

(20) Bain, C. D.; Whitesides, G. M. Depth sensitivity of wetting: monolayers of .omega.-mercapto ethers on gold. *J. Am. Chem. Soc.* **1988**, *110*, 5897–5898.

(21) Busse, L.; Peter, K.; Karl, C. W.; Geisler, H.; Klüppel, M. Reducing friction with Al₂O₃/SiO₂-nanoparticles in NBR. *Wear* **2011**, *271*, 1066–1071.

(22) Liston, E. M.; Martinu, L.; Wertheimer, M. R. Plasma surface modification of polymers for improved adhesion: a critical review. *J. Adhes. Sci. Technol.* **1993**, *7*, 1091–1127.

(23) Karl, C. W.; Lang, A.; Busse, L.; Stoll, A.; Weiße, A.; Stoll, M.; Klüppel, M. Tribological properties of varnished elastomers - part 2: Characterization of stationary friction with smooth surfaces. *KGK, Kautsch. Gummi Kunstst.* **2012**, *65*, 33–36.

(24) Cwikel, D.; Zhao, Q.; Liu, C.; Su, X.; Marmur, A. Comparing Contact Angle Measurements and Surface Tension Assessments of Solid Surfaces. *Langmuir* **2010**, *26*, 15289–15294.

(25) Wu, S. Calculation of interfacial tension in polymer systems. *J. Polym. Sci., Part C: Polym. Symp.* **1971**, *34*, 19–30.

(26) Wu, S. Polar and Nonpolar Interactions in Adhesion. *J. Adhes.* **1973**, *5*, 39–55.

(27) Zgura, I.; Moldovan, R.; Negrila, C. C.; Frunza, S.; Cotorobai, F.; Frunza, L. Surface free energy of smooth and dehydroxylated fused quartz from contact angle measurements using some particular organics as probe liquids. *J. Optoelectron. Adv. Mater.* **2013**, *15*, 627–634.

(28) ISO 25178-2:2012 *Geometrical Product Specifications (GPS)—Surface Texture: Areal—Part 2: Terms, Definitions and Surface Texture Parameters*, 2012.

(29) Karl, C. W.; Klüppel, M. Characterization of Elastomers by Wetting: Roughness and Chemical Heterogeneity. *Chem. Listy* **2011**, *105*, s275–s276.

(30) Nonomura, Y.; Seino, E.; Abe, S.; Mayama, H. Preparation and Characterization of Fractal Elastomer Surfaces. *J. Oleo Sci.* **2013**, *62*, 587–590.

(31) Husein, I. F.; Chan, C.; Chu, P. K. Surface energy and chemistry of ethylene-propylene-diene elastomer (EPDM) treated by plasma immersion ion implantation. *J. Mater. Sci. Lett.* **2002**, *21*, 1611–1614.

(32) Helmy, A. K.; de Bussetti, S. G.; Ferreira, E. A. The water–silicas interfacial interaction energies. *Appl. Surf. Sci.* **2007**, *253*, 6878–6882.

(33) Ross, G. G.; Chass, M.; Bolduc, M. Effect of ageing on wettability of quartz surfaces modified by Ar implantation. *J. Phys. D: Appl. Phys.* **2003**, *36*, 1001–1008.

(34) Zdziennicka, A.; Szymczyk, K.; Jańczuk, B. Correlation between surface free energy of quartz and its wettability by aqueous solutions of nonionic, anionic and cationic surfactants. *J. Colloid Interface Sci.* **2009**, *340*, 243–248.

(35) Meiron, T. S.; Marmur, A.; Saguy, I. S. Contact angle measurement on rough surfaces. *J. Colloid Interface Sci.* **2004**, *274*, 637–644.

(36) Wolansky, G.; Marmur, A. Apparent contact angles on rough surfaces: the Wenzel equation revisited. *Colloids Surf., A* **1999**, *156*, 381–388.

(37) Galuska, A. A. Quantitative ToF-SIMS analysis of monomers, oxidation and trace elements in EPDM gels. *Surf. Interface Anal.* **2001**, *31*, 177–184.

(38) Thøgersen, A.; Selj, J. H.; Marstein, E. S. Oxidation effects on graded porous silicon anti-reflection coatings. *J. Electrochem. Soc.* **2012**, *159*, D276–D281.

(39) Fujishima, M.; Funakoshi, C.; Yoshida, Y.; Yamashita, T.; Kashiwagi, K.; Ishihara, K. Plasma polymerized thin films of organosilicon derivatives and their hydrophobic properties. *Kobunshi Ronbunshu.* **1995**, *52*, 373–377.